J Electr Eng Technol Vol. 9, No. 2: 600-608, 2014
http://dx.doi.org/10.5370/JEET.2014.9.2.600

ISSN(Print) 1975-0102
ISSN(Online) 2093-7423

On-line Parameter Estimation of Interior Permanent Magnet Synchronous Motor using an Extended Kalman Filter

Hyun-Woo Sim*, June-Seok Lee* and Kyo-Beum Lee†

Abstract – This paper presents estimation of d-axis and q-axis inductance of an interior permanent magnet synchronous motor (IPMSM) by using an extended Kalman filter (EKF). The EKF is widely used for control applications including the motor sensorless control and parameter estimation. The motor parameters can be changed by temperature and air-gap flux. In particular, the variation of the inductance affects torque characteristics like the maximum torque per ampere (MTPA) control. Therefore, by estimating the parameters, it is possible to improve the torque characteristics of the motor. The performance of the proposed estimator is verified by simulations and experimental results based on an 11kW PMSM drive system.

Keywords: Parameter estimation, Interior permanent magnet synchronous motor (IPMSM), Extended Kalman Filter (EKF), Maximum torque per ampere (MTPA)

1. Introduction

Permanent magnet synchronous motors (PMSMs) have high efficiency because there is no field winding in the rotor for the generation of the magnetic flux. Also they have better high power density and fast transient response than a dc motor and induction motor. Because of this characteristic of PMSMs, it is widely used in general industrial fields, especially in high-performance motor control applications. PMSMs can be classified into surface-mounted permanent magnet synchronous motors (SPMSMs) and interior permanent magnet synchronous motors (IPMSMs), depending on the arrangement of the permanent magnet. Since the IPMSM has magnet mounted inside the rotor, it is mechanically strong and beneficial for high-speed operation compared with the SPMSM. The inductance difference between d-axis and q-axis of the IPMSM is generated by the location of the mounted permanent magnet. The difference of inductance causes the additional torque called the reluctance torque. For this reason, the torque characteristic and control method of the IPMSM is different from the SPMSM. Therefore, various control methods to take an advantage of the IPMSM have been proposed [1-3].

To improve the torque characteristic of the IPMSM in the constant torque region, the maximum torque per ampere (MTPA) control has been introduced. There are many stator current vectors that generate the constant torque. Among these current vectors, the current of the minimum magnitude is called the MTPA current. The angle of the current vector is changed with the parameter variation because the angle of the minimum current vector relates to d-axis and q-axis inductance. Unfortunately, the stator resistance, inductance and magnet flux are sensitive to the variation of temperature [1-4]. Variation of d-axis and q-axis inductance can decrease effectiveness of the MTPA control and current controller. It means that accurate information of d-axis and q-axis inductance by on-line parameter estimation is necessary to improve motor drives.

Several on-line parameter estimations such as the extended Kalman filter (EKF), recursive least square (RLS), and model reference adaptive system (MRAS) have been proposed [5-10]. Among them, the extended Kalman filter is the most effective estimator in terms of the least-square for estimating the states of nonlinear systems, which is very appropriate for implementation in systems with sensors affected by noise. It processes all the available measure-ments regardless of their accuracy, to provide fast and precise estimation of the target variables, and also accomplish a quick convergence. Moreover, the EKF serves to be appropriate for the state estimation of a PMSM. It appears to be a viable and computationally efficient option for the on-line estimation of the speed, rotor position and parameters. This is feasible because a mathematical model, which describing the motor dynamics is very well known. The terminal quantities like voltages and currents can be measured easily and are appropriate for the determination of the parameters of the machine in an indirect way [7-15].

In this paper, the extended Kalman filter (EKF) based on an on-line identification method is proposed to estimate d-axis and q-axis inductances of the IPMSM. This paper is organized as follows. Firstly, the mathematical model of the IPMSM and MTPA control methods are reviewed briefly. Secondly, the process of a nonlinear system of the IPMSM applied to the EKF is presented. Finally, the

† Corresponding Author: Dept. of Electrical and Computer Engineering, Ajou University, Suwon, Korea. (kyl@ajou.ac.kr)
* Dept. of Electrical and Computer Engineering, Ajou University, Suwon, Korea. (bigle@ajou.ac.kr, junpb@ajou.ac.kr)
Received: August 20, 2013; Accepted: November 28, 2013

simulation and experimental results show the validity of the estimator.

2. Mathematical Model of IPMSM and MTPA Control

2.1 Mathematical model of IPMSM

The three different coordinate systems of IPMSMs are shown in Fig. 1.

Each coordinate transformation is expressed as:

$$\begin{bmatrix} i_\alpha \\ i_\beta \end{bmatrix} = T^t \begin{bmatrix} i_a \\ i_b \\ i_c \end{bmatrix}, \quad \text{with} \quad T = \frac{2}{3}\begin{bmatrix} 1 & 0 \\ -1/2 & \sqrt{3}/2 \\ -1/2 & -\sqrt{3}/2 \end{bmatrix} \tag{1}$$

$$\begin{bmatrix} i_d \\ i_q \end{bmatrix} = P\begin{bmatrix} i_\alpha \\ i_\beta \end{bmatrix}, \quad \text{with} \quad P = \begin{bmatrix} \cos\theta & \sin\theta \\ -\sin\theta & \cos\theta \end{bmatrix} \tag{2}$$

The voltage equation of an IPMSM in the stationary reference frame for an analysis of the stator current is defined as follows:

$$\begin{bmatrix} v_\alpha \\ v_\beta \end{bmatrix} = R_s \begin{bmatrix} i_\alpha \\ i_\beta \end{bmatrix} + p\begin{bmatrix} L-\Delta L\cos 2\theta & -\Delta L\sin 2\theta \\ -\Delta L\sin 2\theta & L+\Delta L\cos 2\theta \end{bmatrix}\begin{bmatrix} i_\alpha \\ i_\beta \end{bmatrix} + \phi_f \begin{bmatrix} \cos\theta \\ \sin\theta \end{bmatrix} \tag{3}$$

where

$$L = \frac{L_q + L_d}{2}, \quad \Delta L = \frac{L_q - L_d}{2}$$

while v_α, v_β and i_α, i_β are the α-axis and β-axis voltages and currents, respectively. L_d and L_q are d-axis and q-axis inductance, ϕ_f is the permanent magnet flux linkage, p is the differential operator and θ is the rotor position.

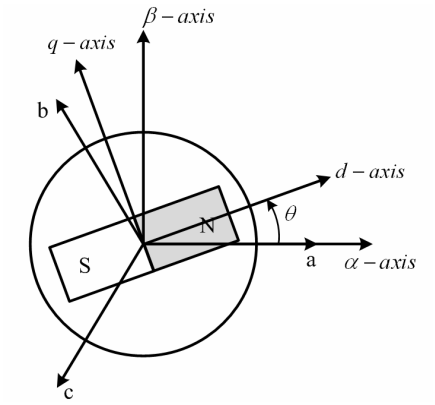

Fig. 1. Coordinate systems of an IPMSM.

The voltage equation in synchronous reference frame can be obtained by

$$\begin{bmatrix} v_d \\ v_q \end{bmatrix} = \begin{bmatrix} R_s + pL_d & -\omega_r L_q \\ \omega_r L_d & R_s + pL_q \end{bmatrix}\begin{bmatrix} i_d \\ i_q \end{bmatrix} + \begin{bmatrix} 0 \\ \omega_r \phi_f \end{bmatrix} \tag{4}$$

where ω_r is the rotor speed in the electric angle.

2.2 Torque characteristic and MTPA control

The magnetic path of an IPMSM is different from that of an SPMSM since the relative permeability of a permanent magnet is nearly equal to the air. This characteristic causes an effect which produces an air-gap on the d-axis.

Because the permanent magnets of the SPMSM are attached to the rotor surface, d-axis inductance is equal to q-axis inductance. Otherwise, in the IPMSM, d-axis inductance is different from q-axis inductance depending on the position of permanent magnets. As shown in Fig. 2, the q-axis inductance is larger than the d-axis inductance because permanent magnets are on the d-axis path where the magnetic flux occurs. The reluctance torque is generated by magnetic saliency from the difference of inductance. Accordingly, the generated torque of the IPMSM consists of the magnetic torque and the reluctance torque as follows [1, 4]:

$$T_e = \frac{3}{2}\frac{P}{2}[\phi_f i_q + (L_d - L_q) i_d i_q] \tag{5}$$

where P is the number of poles.

In (5), there are many pairs of d-axis and q-axis reference currents that generate the same torque. When the reference current is given as the stator current, the torque can be derived as (6). In such a case, the reference d- and q-axis currents are generated by the angle of the stator current.

$$T_e = \frac{P}{2}\frac{3}{2}[\phi_f I_s \sin\theta + \frac{(L_d - L_q)}{2} I_s^2 \sin 2\theta] \tag{6}$$

where θ is the stator current angle in the synchronous reference frame, and I_s is the stator current vector.

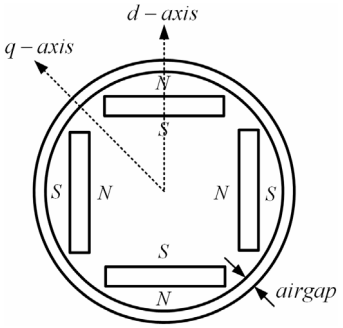

Fig. 2. Rotor structure of an IPMSM (4p)

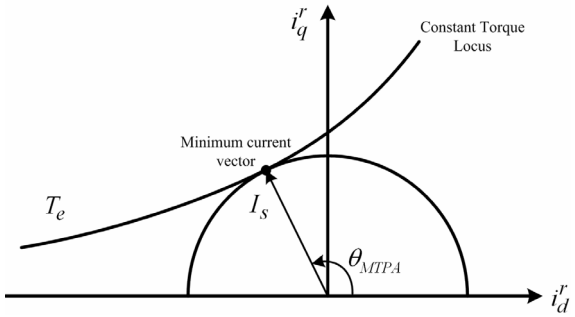

Fig. 3. Constant torque locus and minimum stator current vector

For this reason, there is the minimum stator current that generate the same torque. By operating at the minimum current, maximum torque per ampere (MTPA) is possible.

The constant torque locus on the current plane in the synchronous reference frame is shown in Fig. 3. This figure shows that the MTPA operating point is the nearest point from the origin to the constant torque locus on the current plane. Therefore, the differentiation of the torque with respect to the current angle in the synchronous reference frame, $\partial T_e / \partial \theta$ should be zero at the MTPA point given as follows [1]

$$\frac{\partial T_e}{\partial \theta} = \frac{P}{2}\frac{3}{2}[\phi_f I_s \cos\theta + (L_d - L_q) I_s^2 \cos 2\theta] = 0 . \quad (7)$$

From (7), the current angle of the MTPA control can be derived as

$$\theta_{MTPA} = \cos^{-1}\left(\frac{-\phi_f + \sqrt{\phi_f^2 + 8(L_d - L_q)^2 I_s^2}}{4(L_d - L_q) I_s} \right). \quad (8)$$

By using this angle of the MTPA control, effective d-axis and q-axis reference currents can be expressed as

$$i_d^r = I_s \cos\theta_{MTPA} \ , \ \ i_q^r = I_s \sin\theta_{MTPA} \quad (9)$$

As shown in (8), d-axis and q-axis inductance contribute to the angle of the MTPA control. It means that variation of inductance will not be able to find the optimal MTPA point. For efficient motor drives, the d-axis and q-axis should be estimated.

3. Extended Kalman Filter for Parameter Estimation

An EKF has been used for wide applications in drive control and parameter estimation. In addition, the EKF is useful for a PMSM because it has high-performance in the noisy condition and wide speed control range. Thus, it is often used to acquire the angular speed from noisy mechanical measurements, estimate the rotor position in a mechanical sensorless control application and distinguish the machine parameters. In this section, the latter application for an IPMSM will be given a special attention. The proposed EKF provides estimated d-axis and q-axis inductance [7, 8].

3.1 IPMSM identification model

Eq. (4) can be redefined as follows

$$\begin{aligned} v_d &= R_s i_d + L_d \frac{di_d}{dt} - \omega_r L_q i_q \\ v_q &= R_s i_q + L_q \frac{di_q}{dt} + \omega_r L_d i_d + \omega_r \phi_f \end{aligned} . \quad (10)$$

The system model should be in the form of the state equation to be used in the EKF. The state equations can be expressed as follows

$$\begin{aligned} \dot{\mathbf{x}}(t) &= \mathbf{f}(\mathbf{x}(t)) + \mathbf{G}\mathbf{v}(t) + \sigma(t) \\ \mathbf{y}(t) &= \mathbf{H}\mathbf{x}(t) + \mu(t) \end{aligned} \quad (11)$$

Where $\mathbf{v} = [v_d, v_q]^{\mathrm{T}}$ and $\mathbf{y} = [i_d, i_q]^{\mathrm{T}}$ are input and output vectors. $\mathbf{x} = [i_d i_q \, ab]^{\mathrm{T}}$ is a system state vector (a=1/L_d, b=1/L_q). $\sigma(t)$ and $\mu(t)$ are uncorrelated zero-mean white Gaussian noises with covariance **Q** and **R** respectively. $\sigma(t)$ is system noise that includes the system disturbances and model inaccuracies, while $\mu(t)$ represents the measure-ment noise.

The system matrices **f**(**x**(t)), **G** and **H** are defined as:

$$\mathbf{f}(\mathbf{x}(t)) = \begin{bmatrix} a(-R_s i_d) + \frac{a}{b}\omega_r i_q \\ b(-R_s i_q - \omega_r \phi_f) - \frac{b}{a}\omega_r i_d \\ 0 \\ 0 \end{bmatrix} \quad (12)$$

$$\mathbf{G} = \begin{bmatrix} a & 0 \\ 0 & b \\ 0 & 0 \\ 0 & 0 \end{bmatrix}, \quad \mathbf{H} = \begin{bmatrix} 1 & 0 & 0 & 0 \\ 0 & 1 & 0 & 0 \end{bmatrix} \quad (13)$$

$$\mathbf{F}(x(t)) = \left.\frac{\partial \dot{\mathbf{x}}}{\partial \mathbf{x}}\right|_{\mathbf{x}=\mathbf{x}(t)}$$

$$= \begin{bmatrix} -aR_s & \frac{a\omega_r}{b} & v_d - R_s i_d + \frac{\omega_r i_q}{b} & -\frac{a\omega_r i_q}{b^2} \\ -\frac{a\omega_r}{b} & -bR_s & \frac{b\omega_r i_d}{a^2} & v_q - R_s i_q - \omega_r(\phi_f - \frac{i_d}{a}) \\ 0 & 0 & 0 & 0 \\ 0 & 0 & 0 & 0 \end{bmatrix} \quad (14)$$

The prediction of the state covariance requires the on-line computation of the Jocobian matrix **F**, defined as (14).

3.2 Extended kalman filter

The overall structure of the EKF algorithm consists of two steps called the prediction step and innovation step. The first step performs a prediction of both quantities based on the previous estimates $\hat{\mathbf{x}}_{k-1|k-1}$ and the mean voltage $<\mathbf{v}_{k-1}>$ actually induced to the system in the period from t_{k-1} to t_k. The next step corrects the predicted state estimate and its covariance matrix using a feedback correction scheme that receives the measured motor currents [11].

The common EKF algorithm is expressed following two stages:

1) Prediction step

$$\hat{\mathbf{x}}_{k|k-1} = \hat{\mathbf{x}}_{k-1|k-1} + [\mathbf{f}(\hat{\mathbf{x}}_{k-1|k-1}) + \mathbf{G}\langle \mathbf{v}_{k-1} \rangle]T_s$$

$$\mathbf{P}_{k|k-1} = \mathbf{P}_{k-1|k-1} + (\mathbf{F}_{k-1}\mathbf{P}_{k-1|k-1} + \mathbf{P}_{k-1|k-1}\mathbf{F}_{k-1}^T)T_s + \mathbf{Q}$$

2) Innovation step

$$\hat{\mathbf{x}}_{k|k} = \hat{\mathbf{x}}_{k|k-1} + \mathbf{K}_k(\mathbf{y}_k - \mathbf{H}\hat{\mathbf{x}}_{k|k-1})$$

$$\mathbf{P}_{k|k} = \mathbf{P}_{k|k-1} - \mathbf{K}_k\mathbf{H}\mathbf{P}_{k|k-1}$$

3) Kalman gain

$$\mathbf{K}_k = \mathbf{P}_{k|k-1}\mathbf{H}^T(\mathbf{H}\mathbf{P}_{k|k-1}\mathbf{H}^T + \mathbf{R})^{-1}$$

For the on-line application of the Kalman filter, time constraints are crucial; where most of the matrices hold numerous null elements, all the calculations have been made explicitly, reducing computational time.

A critical step in the design of the Kalman filters is the choice of the initial values for the covariance matrices **Q** and **R** as they influence the performance, convergence and stability. The matrix **Q** is related to the system noise. The rise in the value of the elements of **Q** will likewise raise the Kalman gain, resulting in quicker filter dynamics but with worse the steady-state performance. On the other hand, the matrix **R** is related to the measurement noise. Increasing the values of the elements of **R** will assume that the current measurements are largely influenced by noise and thus less dependable. Therefore, the Kalman gain will decrease, yielding worse transient response. The diagonal initial state covariance matrix $\mathbf{P}_0$ represents variances or mean-squared errors with regard to the initial condition. Varying $\mathbf{P}_0$ yields the different amplitude of the transient, while both transient duration and steady state conditions will be unchanged [12, 13].

In this paper, the initial values of covariance matrix $\mathbf{P}_0$ and system matrix **Q** and **R** have been chosen with a trial-and-error procedure to get the best tradeoff between filter stability and convergence time [8]. As the value of **Q** increases, Kalman gain also increases, which causes variation of estimation values. Likewise, EKF is strongly affected by measurement noise as **R** increases. $\mathbf{P}_0$ is selected based on [8] because it is nothing to do with steady-state condition. In conclusion, to obtain the high performance of proposed EKF, matrices are chosen as follows

$$\mathbf{P}_0 = \begin{bmatrix} 1 & 0 & 0 & 0 \\ 0 & 1 & 0 & 0 \\ 0 & 0 & 300 & 0 \\ 0 & 0 & 0 & 100 \end{bmatrix} \quad \mathbf{Q} = \begin{bmatrix} 0.1 & 0 & 0 & 0 \\ 0 & 0.1 & 0 & 0 \\ 0 & 0 & 10 & 0 \\ 0 & 0 & 0 & 10 \end{bmatrix}$$

$$\mathbf{R} = \begin{bmatrix} 0.5 & 0 \\ 0 & 0.5 \end{bmatrix}.$$

4. Simulation and Experimental Results

4.1 Simulation results

The proposed estimation method was demonstrated by using the PSIM software. The overall system operation is shown in Fig. 4. The current control and speed control are included in the drive system. Estimated inductances by the EKF are used for the current controller to calculate the gain of the current controller.

The simulation studies were operated for the 11kW

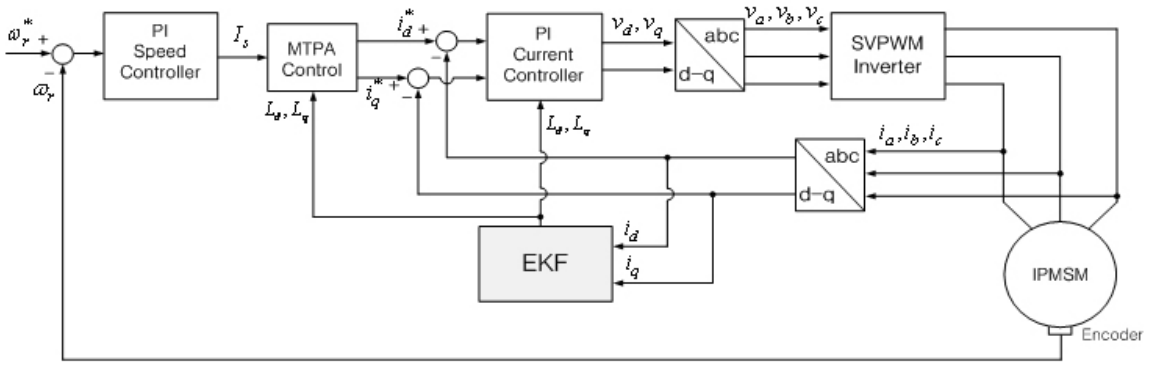

Fig. 4. Configuration of the IPMSM drive system with parameter estimation

Table 1. Motor specifications

Stator Resistance	0.349Ω
d-axis Inductance	13.16mH
q-axis Inductance	15.6mH
Number of poles	6
Flux Linkage	0.554Wb
Rated Power	11kW
Rated Current	19.9A
Rated Speed	1750 rpm

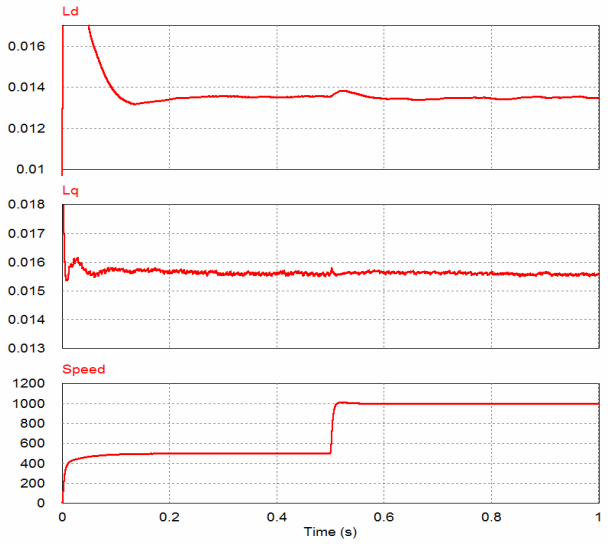

Fig. 5. Parameter estimation with speed variation

IPMSM system. Switching frequency and sampling period T_s are 10 kHz and 100 μs respectively. The simulation was performed in two different conditions of speed at 500 rpm and 1000 rpm. Also, estimated results are confirmed according to the initial inductance value. Initial inductance values were set as 0.5L and 2L. The whole system parameters are given as Table 1.

Fig. 5 shows the results of parameter estimation with speed variation. The good performance of estimation can be confirmed for both 500rpm and 1000rpm. Also, the fast response to step change of speed can be seen through the estimated value.

Results of estimated value according to the initial value of inductance can be seen in Figs. 6 and 7. When starting the operation of motor, initial inductance values are applied to the motor drive. After 0.3s, the EKF starts to estimate parameters used to calculate the gain of the current controller. The estimated values arrive at the steady-state in a very short time within 0.1s, and results show an accurate value. The estimated results show a consistent value with the inductance initial value. Indeed, estimated parameters are the same for the different speed conditions at 500 rpm and 1000 rpm.

Generally, EKF is very appropriate for implementation in systems with sensors affected by noise that is the biggest reason why EKF is used for parameter estimation. To confirm this characteristic for proposed EKF, we tried to

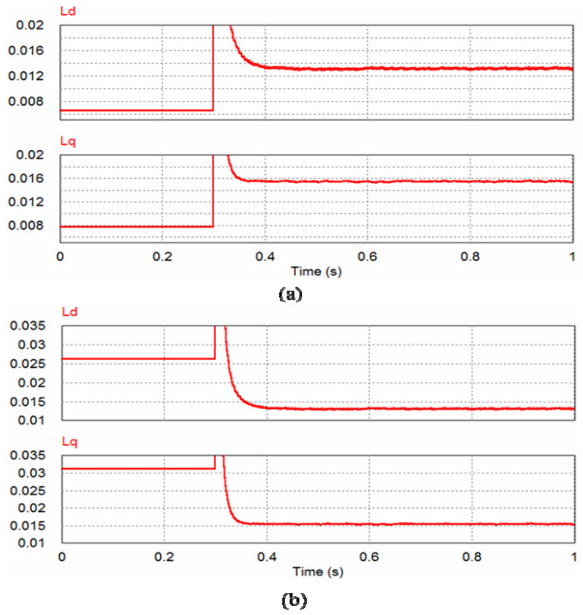

Fig. 6. Parameter estimation at 500rpm with different initial value (a) L_0=0.5L (b) L_0=2L

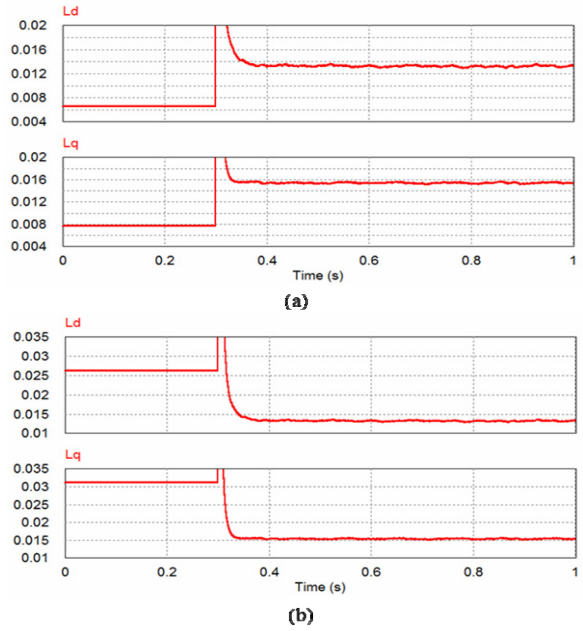

Fig. 7. Parameter estimation at 1000rpm with different initial value (a) L_0=0.5L (b) L_0=2L

compare the EKF and RLS algorithm as shown in Fig. 8. After 0.5s, noise signal is injected to 3-phase current. It can be seen that proposed EKF is not sensitive to noise signal while estimated d-axis inductance from the RLS algorithm is affected by noise signal.

4.2 Experimental results

In order to verify the proposed EKF algorithm, experiments were carried out by using the 11kW IPMSM and TMS320F28335 DSP controller as shown in Fig. 9.

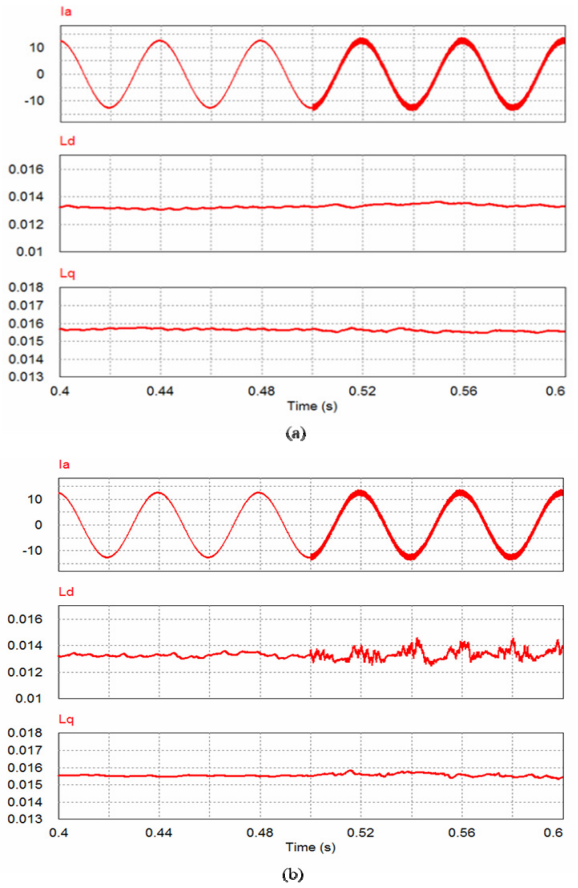

Fig. 8. Comparison of the estimation performance for noise signals: (a) EKF; (b) RLS.

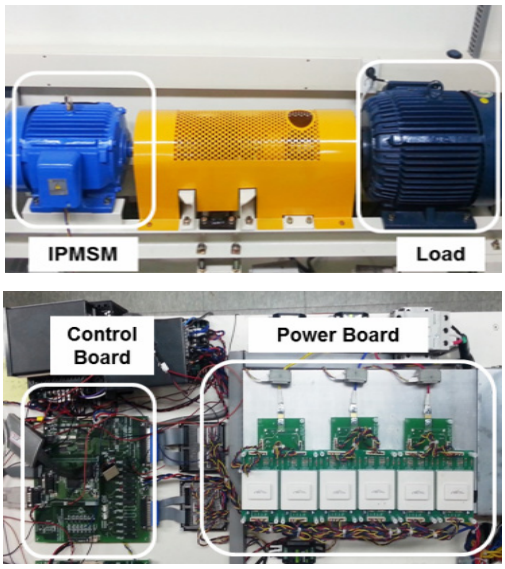

Fig. 9. Experimental setup of IPMSM drive system.

The experiments were performed under the same condition as that of the simulation. The switching frequency and sampling period T_s are 10kHz and 100 μs respectively. The load is the 15kW induction motor. The computation time of the proposed EKF in our bench is about 20 μs, which can be operated within sampling period.

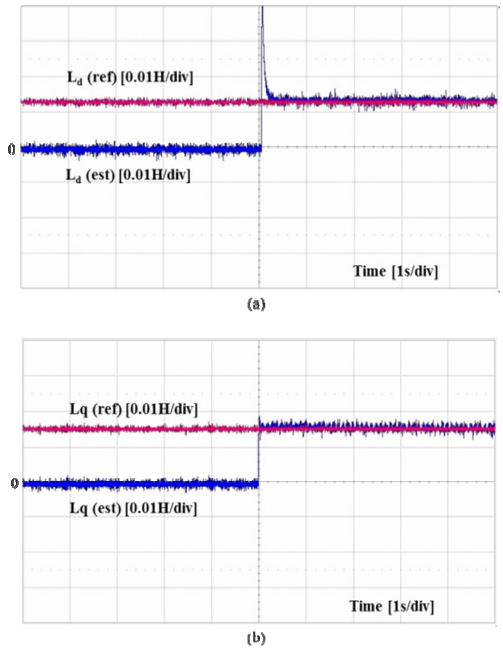

Fig. 10. Experimental results of the parameter estimation at 500rpm with initial values 0.5L (a) $\hat{L}_d$ (b) $\hat{L}_q$

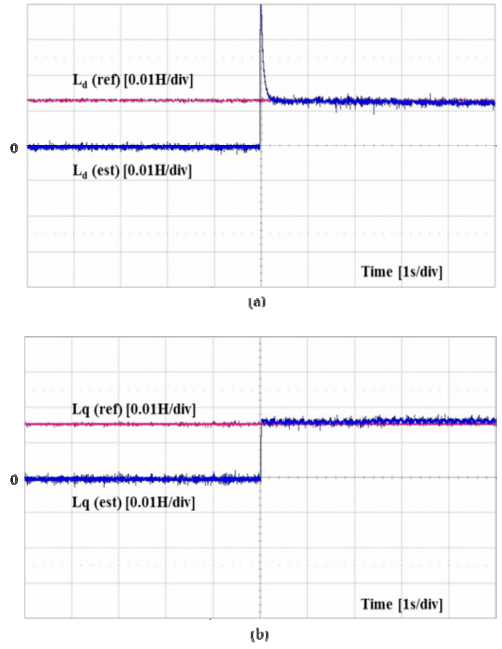

Fig. 11. Experimental results of the parameter estimation at 1000rpm with initial values 0.5L (a) $\hat{L}_d$ (b) $\hat{L}_q$

The experimental results of parameter estimation are shown in Figs. 10 and 11. In these figures, initial values of d- and q-axis inductance were set as 0.5L. In addition, experiments were carried out as two different speed conditions in 500rpm and 1000rpm. Figs. 10 and 11 show the correctly estimated d-axis and q-axis inductance. These experimental results are the same as the simulation results.

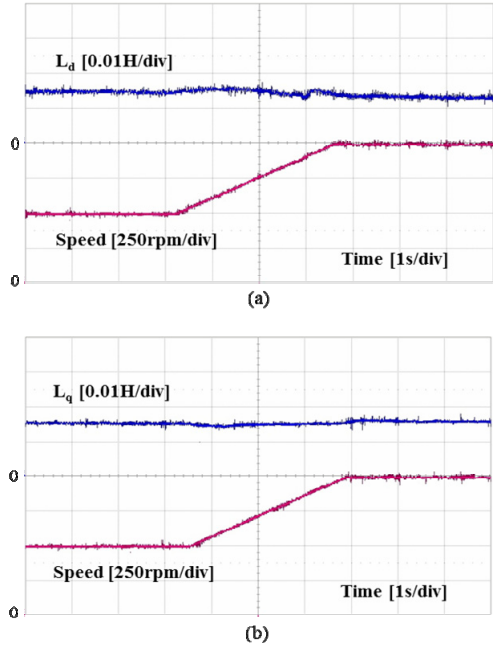

Fig. 12. Experimental results of the parameter estimation with speed variation (a) $\hat{L}_d$ (b) $\hat{L}_q$

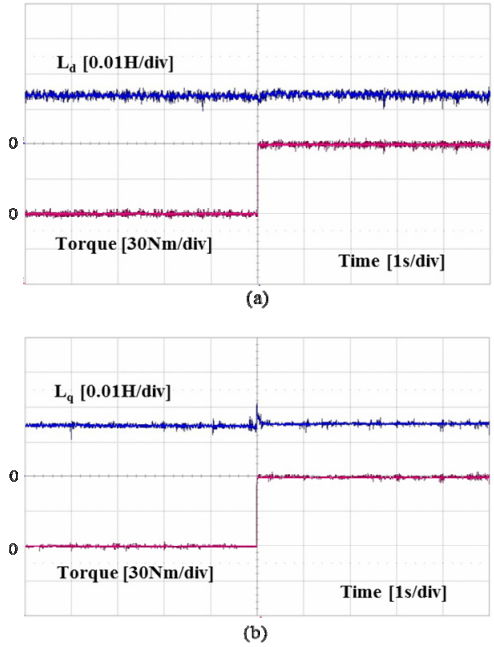

Fig. 13. Experimental results of the parameter estimation with full step load torque (a) $\hat{L}_d$ (b) $\hat{L}_q$

Both simulation and experimental results can see that the convergence time of d-axis inductance is longer than q-axis inductance. This is related to the configuration of the initial matrix value of the EKF.

Fig. 12 shows the performance of parameter estimation when the rotor speed changes from 500rpm to 1000rpm. Fig. 12(a) shows the estimated d-axis inductance that has very small estimation error and it represents the stable response. Moreover, estimated q-axis inductance is more stable than d-axis inductance as shown in Fig. 12(b). For this reason, the performance of the proposed EKF is not sensitive to variable speed.

Also, when the full step load torque is applied to the system, the performance of estimation is maintained and it is presented in Fig. 13. It can be seen from these experimental results that the parameter estimation of the proposed EKF is implemented well regardless of the speed change and variable load torque. From all of the simulation and experiment results, estimation error rate were within 5 percent. In addition, compared with other method, EKF has high-performance estimation accuracy [7].

Figs. 14 and 15 show the MTPA operation with parameter estimation using proposed EKF. To clearly verify the effect of the parameter estimation in the MTPA operation, the difference of the initial inductance value is set to be large that is 10mH and 20mH respectively. Through the parameter estimation during the MTPA operation, it can be seen that the minimum stator current I_s can be obtained that generate the same torque.

Fig. 14(a) shows the d- and q-axes currents and torque during the MTPA operation when the load torque 40% (24 Nm) is applied, while Fig. 14(b) shows the waveform of

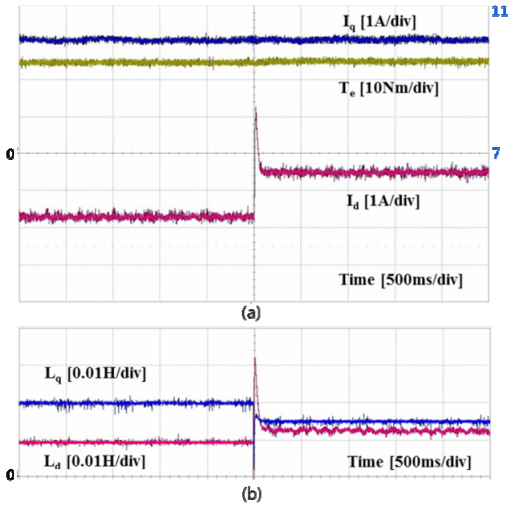

Fig. 14. MTPA operation with parameter estimation under the 40% load.

the changed value of inductance through the parameter estimation at the same time. Since the difference of the initial inductance is large which leads to a large stator current vector angle θ_{MTPA}, it can be seen that a large amount of d-axis current has been flowing. As the parameter estimation is applied, while the torque is at the constant state, the d-axis current decreases while the q-axis current increases but very slightly that it looks almost constant. Hence, because the total stator current value changes from 10.12 A to 10.02 A, which is a decrease of about 0.1 A, it can be known that the minimum current is used to operate. Fig. 15 is the experimental result when the load torque is increased by 80% (48Nm). Similarly, when

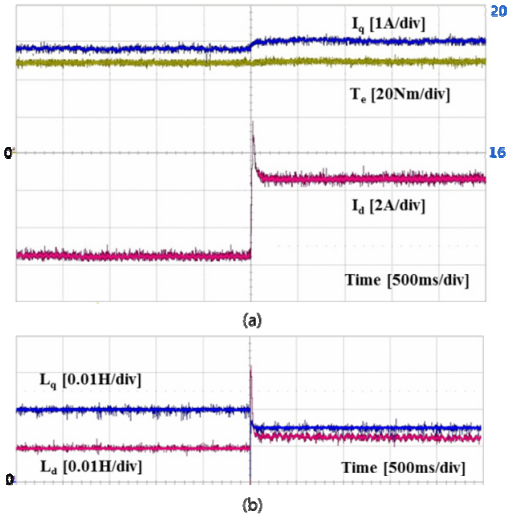

Fig. 15. MTPA operation with parameter estimation under the 80% load.

the parameter estimation is applied, it can be verified that the d-axis is decreased and the q-axis is increased. The total stator current decreased from 19.68 A to 19.15 A, which is about 0.53 A. As the current increases, the MTPA effect increases even more. From the experimental result, the necessity of the parameter estimation for the MTPA operation is verified.

5. Conclusion

This paper proposes a parameter estimation method of the IPMSM using the EKF algorithm. By estimating d-axis and q-axis inductances, it will be able to improve torque characteristic and performance of the controller. Therefore, it will assure the efficient motor drive even if parameters are changed. The validity of the proposed method was demonstrated by simulation and experimental results for various speed and step load torque.

Acknowledgements

This research was supported by Basic Science Research Program through the National Research Foundation of Korea (NRF) funded by the Ministry of Education (2013006090).

References

[1] S. M. Kim, Y. D. Yoon, and S. K. Sul, "Maximum Torque per Ampere (MTPA) Control of an IPM Machine Based on Signal Injection Considering Inductance Saturation," *IEEE Trans. Power Electronics*, vol. 28, no. 1, pp.488-497, Jan. 2013.

[2] J. M. Kim and S. K. Sul, "Speed control of interior permanent magnet synchronous motor drive for the flux weakening operation," *IEEE Trans. Industry Applications*, vol. 33, no. 1, pp. 43-48, Jan./Feb. 1997.

[3] H. Kim, J. Hartwig, and R. Lorenz, "Using on-line parameter estimation to improve efficiency of ipm machine drives," *in 33rd Annual IEEE Power Electronics Specialists Conference, PESC*, vol. 2, pp. 815-820, 2002.

[4] Y. K. Kang, H. G. Jeong, K. B. Lee, D. C. Lee, and J. M. K, "Simple Estimation for Initial Rotor Position and Inductances for Effective MTPA-Operation in Wind- Power systems using an IPMSM," *Journal of Power Electronics*, vol. 10, no. 4, pp. 396-404, July. 2010.

[5] J. W. Kim, K. W. Kim, D. O. Kisck, D. K. Kang, J. H. Chang, and J. M. Kim, "A Study on Sensorless Control of Transverse Flux Rotating Motor Based on MRAS with Parameter Estimation," *Journal of Power Electronics*, vol. 11, no. 6, Nov. 2011.

[6] S. J. Underwood and I. Husain, "Online Parameter Estimation and Adaptive Control of Permanent-Magnet synchronous Machines," *IEEE Trans. Industrial Electronics*, vol. 57, no. 7, pp. 2435-2443, July. 2010.

[7] T. Boileau, B. Nahid-Mobarakeh, and F. Meibody-Tabar, "On-line Identification of PMSM Parameters: Model-Reference vs EKF," *in conf. Rec. IEEE/IAS conf. Annu.*, pp. 1-8, 2008.

[8] T. Boileau, N. Leboeuf, B. Nahid-Mobaraken, and F. Meibody-Tabar, "Online Identification of PMSM Parameters: Parameter Identifiability and Estimator Comparative Study," *IEEE Trans. Industry Applications*, vol. 47, no. 4, pp. 1994-1957, July./Aug. 2011.

[9] K. B. Lee and F. Blaabjerg, "Sensorless DTC-SVM for Induction Motor Driven by a Matrix Converter Using a Parameter Estimation Strategy," *IEEE Trans. Industrial Electronics*, vol. 55, no. 2, pp. 512-521, Feb. 2008.

[10] G. S. Lee, D. H. Lee, T. W. Yoon, K. B. Lee, J. H. Song, and I. Choy, "Speed and Flux Estimation for an Induction Motor Using a Parameter Estimation Technique," *IJCAS(International Journal of Control, Automation, and Systems)*, vol. 3, no. 1, pp.79-86, Mar. 2005.

[11] S. Bolognani, R. Oboe, and M. Zigliotto, "Sensorless full-digital PMSM drive with EKF estimation of speed and rotor position," *IEEE Trans. Industrial Electronics*, vol. 46, no. 1, pp.184-191, Feb. 1999.

[12] S. Bolognani, L. Tubiana and M. Ziglitto, "Extended Kalman Filter Tuning in Sensorless PMSM Drives," *IEEE Trans. Industry Applications*, vol. 39, no. 6, Nov./Dec. 2003.

[13] R. Dhauadi, N. Mohan, and L. Norum, "Design and implementation of an extended kalman filter for the state estimation of a permanent magnet synchronous motor," *IEEE Trans. Power Electronics*, vol. 6, no. 3,

pp. 491-497, Jul. 1991.
[14] D. H. Ha, C. S. Lim and D. S. Hyun, "Robust Optimal Nonlinear Control with Observer for Position Tracking of Permanent Magnet Synchronous Motors," *Journal of Power Electronics*, vol. 13, no. 6, pp. 975-984, Nov. 2013.
[15] H. G. Park, R. Y. Kim and D. S. Hyun, "Open Circuit Fault Diagnosis Using Stator Resistance Variation for Permanent Magnet Synchronous Motor Drives," *Journal of Power Electronics*, vol. 13, no. 6, pp. 985-990, Nov. 2013.

Hyun-Woo Sim received the B.S. degree in Electrical and Computer Engineering from Ajou University, Suwon, Korea, in 2013. He is currently working toward the M.S degree at Ajou University, Suwon, Korea. His research interests include electric machine drives and multilevel inverter and reliability.

June-Seok Lee received the B.S. and M.S. degrees in Electrical and Computer Engineering from the Ajou University, Korea, in 2011 and 2013, respectively. He is currently working toward the Ph.D. degree at Ajou University, Korea. His research interests include grid-connected systems, multilevel inverter and reliability.

Kyo-Beum Lee received the B.S. and M.S. degrees in electrical and electronic engineering from the Ajou University, Korea, in 1997 and 1999, respectively. He received the Ph.D. degree in electrical engineering from the Korea University, Korea in 2003. From 2003 to 2006, he was with the Institute of Energy Technology, Aalborg University, Aalborg, Denmark. From 2006 to 2007, he was with the Division of Electronics and Information Engineering, Chonbuk National University, Jeonju, Korea. In 2007 he joined the Department of Electrical and Computer Engineering, Ajou University, Suwon, Korea. He is an associated editor of the IEEE Transactions on Power Electronics and the Journal of Power Electronics. His research interests include electric machine drives, renewable power generations, and electric vehicles.